Lawrence Berkeley National Laboratory
Recent Work

Title

WHERE HAS ALLTHE FUSION GONE . . . ?

Permalink

https://escholarship.org/uc/item/9vc9214z

Authors

Plagnol, E.
Vinet, L.
Bowman, D.R.

Publication Date

1988-08-01

Lawrence Berkeley Laboratory
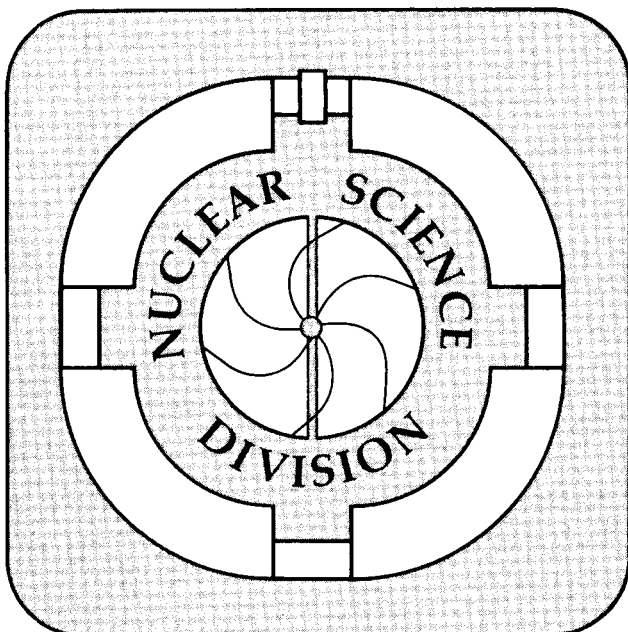## UNIVERSITY OF CALIFORNIA

DEC 2 1988

Where Has All the Fusion Gone . . . ?

E. Plagnol, L. Vinet, D.R. Bowman, Y.D. Chan,
R.J. Charity, E. Chavez, S.B. Gazes, H. Han,
W.L. Kehoe, M.A. McMahan, L.G. Moretto,
R.G. Stokstad, G.J. Wozniak, and G. Auger

August 1988

DISCLAIMER

Where Has All The Fusion Gone...?

E. Plagnol[1], L. Vinet[2], D. R. Bowman, Y. D. Chan, R. J. Charity[3], E. Chavez[4],
S. B. Gazes[5], H. Han[6], W. L. Kehoe[7], M. A. McMahan, L. G. Moretto,
R. G. Stokstad, and G. J. Wozniak

*Nuclear Science Division, Lawrence Berkeley Laboratory, University of California,
Berkeley, California 94720*

G. Auger[8]
Chemistry Department, SUNY, Stony Brook, New York 11794

Abstract:

Charge distributions, kinetic energy spectra, and angular distributions were measured for the reverse kinematics reactions, 19.7 MeV/nucleon ^{40}Ar + ^{12}C & ^{27}Al. Invariant cross section plots constructed in the $V_{||}$ - $V_{\perp}$ plane give a global view of the several competing reaction mechanisms. The evaporation residue cross section, which dominates the fusion cross section for the ^{40}Ar + ^{12}C reaction, decreases dramatically in the ^{40}Ar + ^{27}Al reaction and is replaced by isotropic binary decay, arising presumably from compound nucleus decay.

[1]Present address: GANIL - B.P. 5027 - 14021 CAEN Cedex, FRANCE.
[2]Present address: CERN, Division EP, Ch-1211, Geneva 23, Switzerland.
[3]Present address: Gesellschaft für Schwerionenforschung, 6100 Darmstadt, West Germany
[4]Permanent address: Instituto de Fisica UNAM, A.P. 20364, Mexico, 01000, D.F. Mexico
[5]Present address: Department of Physics, University of Rochester, Rochester, NY.
[6]Permanent address: Institute of Atomic Energy, Beijing, China.
[7]Present address: Department of Chemistry, University of Maryland, College Park, MD 20742
[8]Present address: Institut de Physique Nucleaire, B. P. N$^{\circ}$ 1, 91406 Orsay, FRANCE.

At low excitation energies, the decay of compound nuclei proceeds mainly through a limited number of well defined channels: light particle evaporation, γ rays, and, for heavy nuclei, fission. This is well understood in terms of compound nucleus theory in which the dominant channels are those whose barriers are most comparable to the nuclear temperature. Nuclei can now be produced with much higher excitation energies, and the very same compound nucleus theory indicates that a greater variety of channels, ranging from symmetric fission to light fragment evaporation, should open up and compete effectively with the more traditional channels[1,2]. Consequently, at high enough excitation energies or angular momenta a significant amount of the fusion cross section should be associated with "*complex fragments*" produced in the decay of the compound nucleus or its products. This has already been observed in experiments[3-7] for relatively heavy systems in which all the mass asymmetries ranging from light particle emission to symmetric splitting of the compound nucleus are represented.

In light systems the evaluation of fusion cross sections has been made traditionally by measuring[8,9] the "evaporation residue cross section". The substantial onset of statistical binary decay in competition with the evaporation residue cross section may create an apparent disappearance of the fusion cross section with increasing bombarding energy[10-13]. Consequently, it seems important to determine systematically the cross sections for 1) evaporation residues; 2) isotropic (or compound nucleus-like) binary products; 3) non isotropic binary (quasi-elastic or deep inelastic) products. This separation of the cross section is a prerequisite to any attempt to interpret the reaction mechanism.

The present letter reports on a series of experiments performed at the 88-Inch Cyclotron of the Lawrence Berkeley Laboratory on the $^{40}Ar + {}^{12}C$ and the $^{40}Ar + {}^{27}Al$ systems at 19.7 MeV/nucleon. In the case of complete fusion, the compound nuclei formed in these reactions are ^{52}Cr and ^{67}Ga with excitation energies of 200 and 340 MeV, respectively. Large differences in the excitation energy and angular momentum of the complete or incomplete fusion products are expected and suggest possible dramatic differences in the role of binary decay in the two systems.

In order to have a "global" picture of these reactions, the experiments were

designed to detect both the fusion residues resulting from the evaporation of light particles ($Z \leq 2$) alone, as well as the products associated with the statistical emission of heavier fragments ($Z \geq 5$) from the compound nucleus. One of the advantages of studying such light systems, especially when using the reverse kinematics technique is that the whole range of reaction products can be identified with a standard ΔE-E telescope.

The reaction products were detected in two ΔE(gas) - E(silicon) telescopes ($\Delta \Theta = 5^\circ$). Each telescope consisted of a position-sensitive ionization chamber (ΔE) backed by a 2 mm thick position-sensitive silicon (E) detector. The ionization chambers were operated at 50 mbar of pressure (CF_4) so that heavy fragments emitted from the fast moving compound nuclei produced in the reverse kinematics reaction could be detected with high efficiency. The telescopes were positioned on both sides of the beam so that singles and coincidence events could be recorded. Energy calibrations were obtained by the elastic scattering of ^{40}Ar and ^{12}C beams from a gold target.

To obtain a global view of the cross section, for each element, the invariant cross section has been plotted in the $V_{\parallel}$ (parallel), $V_{\perp}$(perpendicular) plane (see Fig. 1). This required the measurement of a <u>continuous</u> angular distribution from 2.5° to $\sim 60^\circ$ in the laboratory. The laboratory velocities were inferred from the measured energy and Z-value by assuming[4] the mass (A) of the nucleus to be $A = Z*(2.08 + 0.0029*Z)$. Our detection system had two natural limitations: a small threshold in velocity (energy) and the inability to reach very small angles relative to the beam ($\Theta_{lab} \leq 2.5^\circ$) which resulted in a Z-dependent cut-off observed for low velocities (~ 1 cm/ns) and a cut-off around the beam axis, respectively.

Some representative examples of these plots for fragments with Z = 6, 8, 12, and 16 are shown (see Fig. 1) for the ^{40}Ar + ^{12}C and the ^{40}Ar + ^{27}Al systems at 19.7 MeV/nucleon. Particularly instructive is the result obtained for Z = 8 fragments from the ^{40}Ar + ^{12}C system. The binary production of fragments results in a characteristic Coulomb ring, which remains even if it is followed, or preceeded, by a significant amount of light particle evaporation. The very noticeable Coulomb rings observed for this and other Z values result from this quasi two-body kinematics. These Coulomb

rings are centered around the velocities expected for complete fusion events (see Fig. 1). For the fully relaxed events, the binary nature of the reaction has been verified by coincidence measurements in which, for all mass asymmetries, the fragments charges were found to sum to a constant value.

For the ^{40}Ar + ^{12}C system, one can see examples where contributions of other reaction mechanisms can be identified: target-like incompletely damped events (Z = 6, at low velocities) and evaporation residues (Z = 16). For the ^{40}Ar + ^{27}Al reaction, the above patterns differ somewhat from those for the ^{40}Ar + ^{12}C reaction. For example, quasielastic projectile-like events are seen for Z = 16 at high velocities. The most striking differences are the stretching of the patterns along the $V_{\parallel}$ direction and the broadening of the distributions along $V_{\perp}$. The former effect is most likely due to the broader range of incomplete fusion prevailing in this reaction, while the latter seems to be due to the increasing importance of binary decay for the ^{40}Ar + ^{27}Al system.

For the components centered near the center-of-mass velocity, the contour plots in Fig. 1 indicate that, for both systems, isotropic binary decay products dominate for lighter Z values (Z ~ 6 & 8) whereas evaporation residues tend to predominate for heavy products (Z ≥ 16). For intermediate Z-values, both components are present, which can be separated by means of a more detailed analysis (see below).

At higher and lower velocities (projectile-like and target-like fragments, respectively), non isotropic components corresponding to incompletely damped collisions (quasi elastic or deep inelastic) are also present. Although the deep inelastic products and isotropic binary fusion products can be energetically degenerate, deep inelastic products are typically forward or backward peaked, whereas the binary decay products have approximately isotropic angular distributions in the $V_{\parallel}$ and $V_{\perp}$ plane (see Fig. 1, Z = 6 and 8).

In order to extract the cross sections associated with fusion events (both evaporation residues and isotropic binary components), the incompletely relaxed and non isotropic components must be subtracted. To a large extent, the problem of the subtraction and the complications associated with the broad range of incomplete fusion, especially visible in ^{40}Ar + ^{27}Al system, can be removed by projecting on the $V_{\perp}$

plane the forward portion of the distribution for each target-like fragment and the backward portion of the distribution for each projectile-like fragment. In this way distributions in $V_\perp$ were obtained as shown in Fig. 2. For both systems, the distributions broaden substantially and the peaks increase to larger values of $V_\perp$ with decreasing Z value as the binary component becomes more dominant. In addition, the widths are substantially larger for the Al target, presumably due to an increased amount of binary decay.

For the multiple emission of light particles (Z ≤ 2), the distribution of events should be isotropic in the center of mass. The projection of $V_\perp$ is a function of the type:

$$f_{ER}(V_\perp)\,dV_\perp = N_{ER}\exp\left[\frac{-V_\perp^2}{2\sigma_{ER}^2}\right]V_\perp\,dV_\perp \tag{1}$$

where σ_{ER}^2 is the mean square recoil velocity associated with particle evaporation. On the other hand, for a heavy fragment emission (Z > 5), the distribution of events should be isotropic in the reaction plane. The projection on $V_\perp$ yields:

$$f_B(V_\perp)\,dV_\perp = N_B\int\exp\left[-\frac{\left[(V_\perp^2 + V_\parallel^2)^{1/2} - V_o\right]^2}{2\sigma_B^2}\right]dV_\parallel\,dV_\perp \tag{2}$$

where V_o is the mean center-of-mass velocity associated with the binary decay and σ_B^2 is a combination of the fluctuations in the center-of-mass velocity and of the recoil velocity associated with the particle evaporation. For each Z value, Eqs. 1 & 2, which have a total of five unknown parameters, were fit to the experimental distributions in Fig. 2 with a computer code that minimized chi-square. The extracted V_o parameter shows a dependence upon the fragment Z-value which is characteristic of the Coulomb interaction.

As mentioned above, the projected distributions for the ^{12}C and ^{27}Al targets (see Fig. 2) contain only evaporation residues and compound nucleus-like binary decay products. Although the shapes of these distributions change dramatically with Z-value,

they are well reproduced by the sum of the calculated evaporation residue and binary decay distributions, where the fraction of the two components was varied smoothly with increasing Z-value. Examples of the decomposition of the cross section into evaporation residue and binary components are shown in Fig. 2, for a variety of elements. For the ^{40}Ar + ^{12}C reaction, Z = 8 is pure binary and Z = 20 is a pure evaporation residue, whereas Z = 12 is roughly an equal mixture. In contrast, for the ^{40}Ar + ^{27}Al reaction the binary component dominates for most Z values.

The quantitative results from the decomposition of the isotropic components are shown in Fig. 3. The shaded areas correspond to the binary components while the white areas correspond to the evaporation residues. For both targets, one observes that the yield of binary decay is quite important in the intermediate Z region (6 - 12). However, while for the ^{40}Ar + ^{12}C system the evaporation residue yield appears to be dominant at large Z values, this is not the case for the ^{40}Ar + ^{27}Al system, where binary decay seems to dominate at all Z values. This result is quite striking and indicates that, at the higher excitation energies and angular momenta associated with the latter system, even the fragments with Z ≥ 16 (ordinarily believed to arise from light particle evaporation) are also strongly populated by binary decay. A corollary of this conclusion is that residues produced by the evaporation of particles with Z ≤ 2 may represent but a limited fraction of the overall fusion cross section.

Because of the large excitation energies, this binary process is not pure and is followed or possibly preceded by substantial light particle evaporation (n, p, alphas). For this reason the observed secondary Z distribution may be far removed from the initial symmetric charge distribution that is expected from the primary binary decay. This is particularly true for the highly excited light systems under consideration. It can be estimated, for example, that the observation of a Z = 8 nucleus could correspond to an initial symmetric fission of the compound nucleus, where subsequently the two hot fragments lose substantial mass due to sequential light particle emission. At even higher energies, only fragments with very low Z values would remain as the ashes of this very drastic cooling process.

In conclusion, we have shown that both evaporation residues and binary decay products originating from fusion-like products are present in reactions of ^{40}Ar on ^{12}C

and ^{27}Al at 19.7 MeV/nucleon. Evaporation residues dominate for the ^{40}Ar + ^{12}C system whereas binary products dominate for the ^{40}Ar + ^{27}Al system. For the latter system, the large excitation energy of the fusion-like products and higher angular momentum result in a very large probability for binary decay. Thus "standard" evaporation residues (produced by light particle emission ($Z \leq 2$) alone) are strongly depleted by the competing binary decay channels. This disappearance of evaporation residues should not be interpreted as the vanishing of fusion-like products. At even higher excitation energies, sequential binary decay of fusion-like products should lead to ternary and quaternary events.[2] Thus, the observation of three or four bodies at high energies may also be consistent with fusion-like processes.

Acknowledgment

References

1. L. G. Moretto, Nuclear Physics **A247** (1975) 211.

2. L. G. Moretto and G. J. Wozniak, Prog. in Part. and Nucl. Phys. **21** (1988).

3. R. J. Charity et al., Phys. Rev. Lett. **56** (1986) 1354.

4. R. J. Charity et al., Nucl. Phys. **A476** 516 (1988).

5. D. R. Bowman et al., Phys. Lett. **189** (1987) 282.

6. R. J. Charity et al., Nucl. Phys. **A483** (1988) 371.

7. F. Auger et al., Phys. Rev. **35C** (1987) 190.

8. R. G. Stokstad, "The Use of Statistical Models in Heavy-Ion Reaction Studies", Treatise on Heavy-Ion Science, Vol. 3. Ed. D. A. Bromley, Plenum 1985, p.83.

9. G. Auger et al., Z. Phys. **A321** (1985) 243.

10. G. Auger et al., Physics Lett. **169B** (1986) 161.

11. B. Borderie and M. F. Rivet, Z. Phys. **A321** (1985) 703.

12. K. Grotowski et al., Phys. Rev. **C30** (1984) 1214.

13. J. Brzychczyk et al., Phys. Lett. **B194** (1987) 473.

Figure Captions

Fig. 1. Two dimensional contour plots $(d^2\sigma/dV_{||}dV_{\perp})$ in the $V_{||}$ vs $V_{\perp}$ plane for representative Z-values (Z = 6,8,12 &16) from the 20 MeV/nucleon ^{40}Ar + ^{12}C/^{27}Al reactions. The beam direction and the c.m. velocity are indicated by horizontal and vertical arrows, respectively. In general, complete distributions have been measured, except at very low velocities (see e.g. Z = 6) and at very forward angles close to the beam due to the experimental detection limits.

Fig. 2. Projections on the $V_{\perp}$ axis for fragments with representative Z values from the 20 MeV/A ^{40}Ar + ^{12}C/^{27}Al reactions. The shapes of the experimental distributions (histograms) change dramatically with Z-value and are well reproduced by simple calculations for either an evaporation residue (curve - ER) or a binary decay (curve - B) or the sum (curve S) of these two components (see text).

Fig. 3. Extracted yields of evaporation residues (white) and binary decay products (shaded) for the 20 MeV/nucleon ^{40}Ar + ^{12}C/^{27}Al reactions. The excitation energies of the compound nuclei ^{52}Cr and ^{67}Ga are 200 and 340 MeV, respectively.
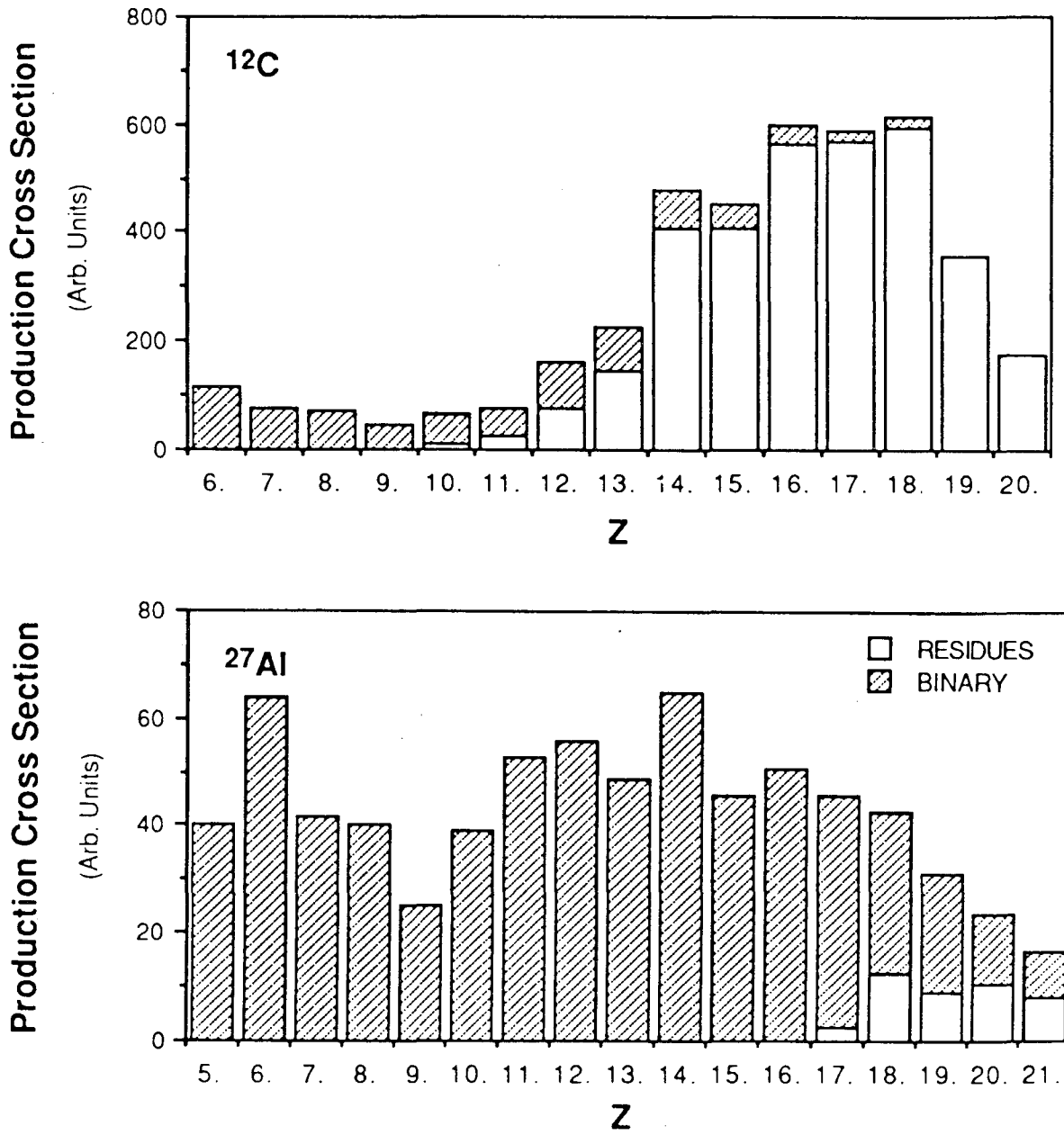
$$^{40}Ar \; (\; 20 \; MeV/A \;) + \; ^{12}C$$

$$^{40}Ar \; (\; 20 \; MeV/A \;) + \; ^{27}Al$$
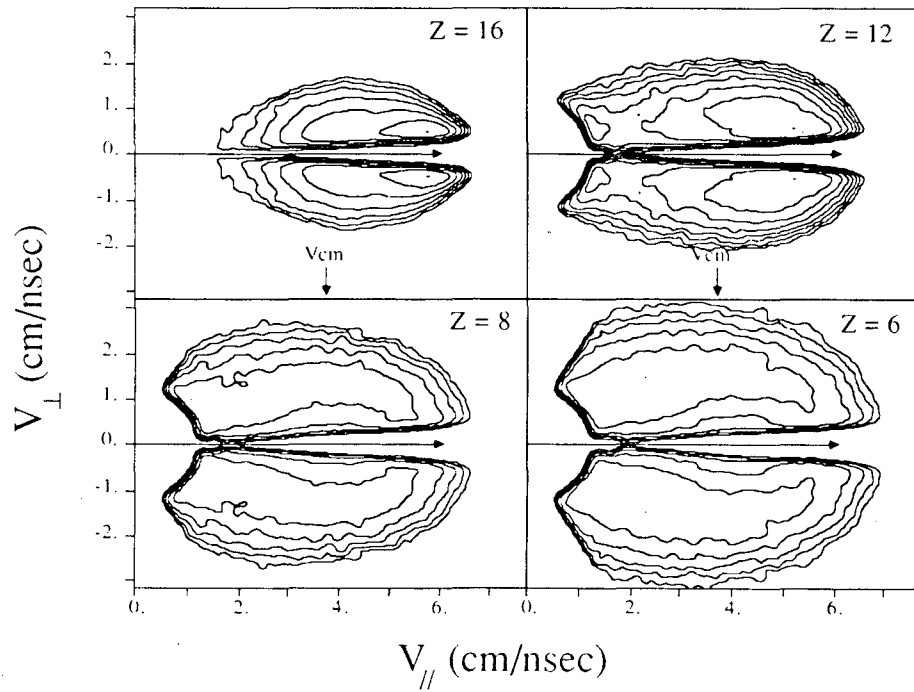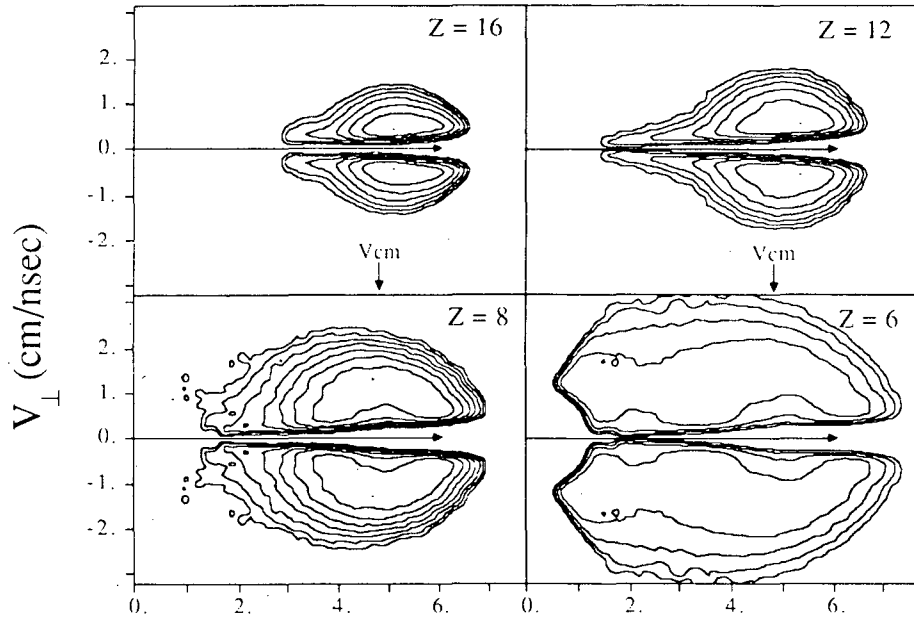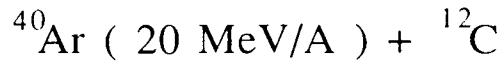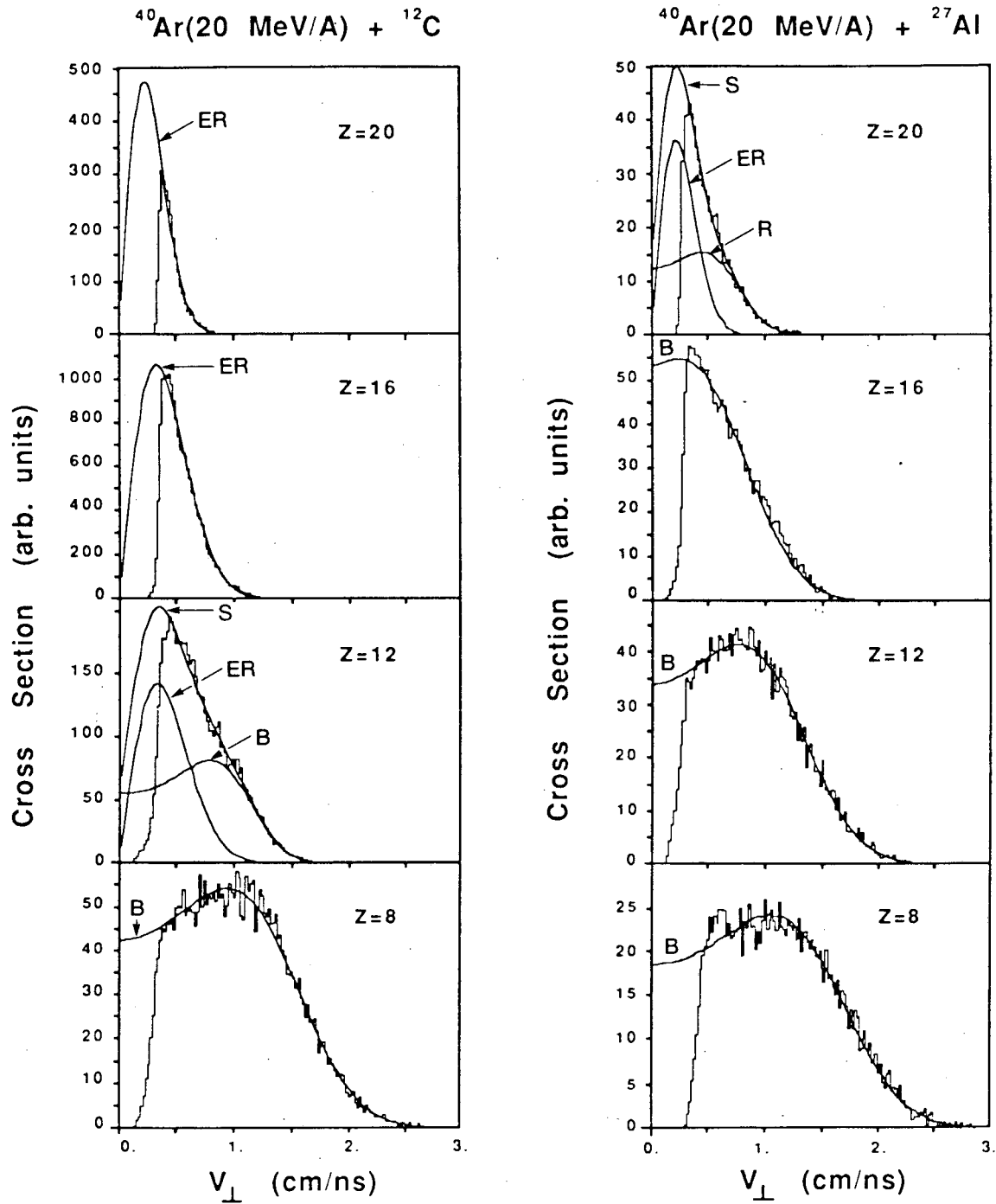
XBL 888-2736A

Figure 1

Figure 2

20 MeV/nucleon ^{40}Ar +

XBL 888-2738A

Figure 3